

# Feedforward Active Noise Control With a New Variable Tap-Length and Step-Size Filtered-X LMS Algorithm

Dah-Chung Chang, *Member, IEEE*, and Fei-Tao Chu

**Abstract**—The fixed tap-length and step-size filtered-X least mean-square (FxLMS) algorithm is conventionally used in active noise control (ANC) systems. A tradeoff between the performance and the convergence rate is a well-known problem due to the choice of the step size. Although the variable-step-size FxLMS algorithms have been proposed for fast convergence, a long tap-length filter is frequently required in order to deal with different environments such that the convergence rate is still subject to a small step size for the long tap length. In this paper, we study a new ANC system with a variable tap-length and step-size FxLMS algorithm. Based on the assumption of an unsymmetric and two-sided exponential decay response model for the ANC control filter, the new FxLMS algorithm has the minimum mean-square deviation for the optimal filter coefficients. In the online secondary path modeling ANC system, simulation results show that the new algorithm with different kind of variable step sizes can provide significant improvements of convergence rate and noise reduction ratio, compared to the fixed-tap-length FxLMS algorithms.

**Index Terms**—Active noise control, exponential decay response, filtered-X LMS, mean-square deviation, noise reduction ratio, secondary path model.

## I. INTRODUCTION

AS IT dates back to at least three decades ago, the acoustic noise reduction problem has been explored for real-life applications such as headphones, automobiles, mobile phones, and some industries which need to remedy the noisy circumstances [1], [2]. Thanks to the rapid development of digital technologies, the active noise control (ANC) systems using adaptive filters may have smaller volume [3] and can be appealing alternatives to those using passive methods. To cancel the undesired noise from a primary noise source, the adaptive ANC algorithms compensate for the uncertain effects in the secondary path, modeling the electrical signal transmission path between the reference microphone and the error microphone, to mini-

mize the cancellation error signal detected by the error microphone. One of most widely used algorithms for the adaptive ANC system is the filtered-X least mean-square (FxLMS) algorithm [4]. Although some adaptive algorithms such as the filtered-X recursive least-squares (FxRLS) [5] and Kalman filter [6] can provide better convergence rate and performance, the FxLMS algorithm is very appealing to researchers because of a relatively lower computational burden.

Some variants of the FxLMS algorithms for ANC can be found in the literature, such as the lattice ANC [7], frequency-domain ANC [8], [9], delayless subband ANC [10], [11], etc. The lattice structure filter fails to provide a satisfying convergence rate when the primary noise is broadband. Taking into account long impulse responses of the primary and the secondary paths, the LMS processing in the transform-domain or subband takes the advantage of a reduced eigenvalue spread of the input autocorrelation matrix so as to obtain a faster convergence rate than the conventional time-domain processing. Nevertheless, the transform-domain algorithm requires an additional complexity to implement the discrete-time Fourier transform (DFT), wavelet, or filter banks. Compared with the above variants, the fixed-step-size FxLMS algorithm is relatively simple from the aspect of implementation. Although the performance and the convergence rate of the ANC control filter can be determined by adjusting the step size, the fixed-step-size algorithm suffers from how to choose a proper step size to fit a variety of environments. As a result, to possess fast convergence, the variable-step-size and the normalized LMS algorithms are tailored for the FxLMS based ANC applications [12]–[14]. However, another practical issue for the ANC application is that the tap length of the ANC filter is usually unknown and may vary in different situations. To accommodate most cases, a priori long-tap-length is required for a fixed-tap-length FxLMS algorithm. This leads to that the maximum step size is limited by a long tap-length ANC filter, and so is the convergence rate [12], [15].

For some applications such as headphone, the plant and the secondary path do not change drastically and offline measurement can be sufficiently applied in these cases. However, for broad ANC applications, the unknown electro-acoustic plant can be considered as dynamic [16], [17]. Moreover, a lot of works, for example [12], [13], [18]–[22], are focused on the on-line modeling and estimation problems. That means, a time-varying plant or secondary path can lead to a time-varying control filter, and hence, we study a new ANC method with a variable tap-length and step-size FxLMS algorithm, maintaining

Manuscript received July 13, 2013; revised October 06, 2013; accepted December 13, 2013. Date of publication January 02, 2014; date of current version January 10, 2014. This work was supported in part by the National Science Council of Taiwan under Contracts NSC 102-2221-E-008-007. The associate editor coordinating the review of this manuscript and approving it for publication was Prof. Woon-Seng Gan.

D.-C. Chang is with the Department of Communication Engineering, National Central University, Taoyuang 32001, Taiwan (e-mail: dcchang@ce.ncu.edu.tw).

F.-T. Chu is with Foxlink Image Technology CO., Ltd. Taipei 236, Taiwan (e-mail: jeff123chu@gmail.com).

Color versions of one or more of the figures in this paper are available online at <http://ieeexplore.ieee.org>.

Digital Object Identifier 10.1109/TASLP.2013.2297016

fast convergence and better performance. There are some existing variable tap-length LMS algorithms [23]–[27] for system identification. Some works [26], [27] considered the exponential decay response for the plant with unknown impulse response since it is the asymptotic behavior in response to many single exponential decay curves in the physical world, and thus, the exponential model can cover a large set of physical systems. For ANC applications, the secondary path commonly includes a lowpass filter that results in a two-sided decaying envelop on the impulse response. Moreover, the maximum impulse response output of the primary plant is not necessarily at the beginning of the response because of acoustic transmission delay in the acoustic duct. Hence, the proposed algorithm in this paper is developed based on an unsymmetric and two-sided exponential decay impulse response model, which is different from the single exponential decay response model previously studied in [26], [27]. The principle of the variable-tap-length algorithm is to first approach the modeled part of the impulse response with a smaller tap length and a larger step size obtained by minimizing the mean-square deviation (MSD) of the filter coefficients. Then, the tap length is progressively increased and finally converged to retain the minimum MSD while continuously decreasing the step size. A new variable-step-size method is also proposed in this paper, with the help of converging to the minimum MSD. Besides, we develop a recursive form for optimal tap-length and step-size estimation in order to simplify the computational complexity. Since the MSD of the two-sided exponential decay model can be proved as a convex function of the tap lengths and step sizes, the new algorithm has the property of global optimality.

The new variable-tap-length FXLMS algorithm is derived based on a generalized form of two different step sizes for the two-sided responses. Furthermore, some practical considerations of the proposed algorithm used in the ANC system are discussed. To verify the performance, we simulate the ANC structure with online secondary path model estimation [18], [28]. The numerical analysis includes the MSD evaluation for a given ANC control filter and the noise reduction ratio (NRR) comparison with the modeling data taken from [2]. Simulation results show that the new variable-tap-length FxLMS algorithm has fast convergence and better performance employed with different kind of variable step sizes, compared to the conventional fixed-tap-length FxLMS algorithms even assuming the tap length can be known a priori.

This paper is organized as follows. Section II provides the development of the new FxLMS algorithm and the recursive form. The global convergence property and application issues in ANC systems are also discussed in this section. Section IV provides numerical comparison of the proposed algorithm with different variable step sizes and other fixed-tap-length FxLMS algorithms. Finally, conclusions are drawn in Section V.

## II. THE ANC SYSTEM USING THE FXLMS ALGORITHM

### A. FxLMS for ANC

A basic ANC structure using the FxLMS algorithm is depicted in Fig. 1(a).  $P(z)$  is an unknown plant in the primary path which models the acoustic response between the reference

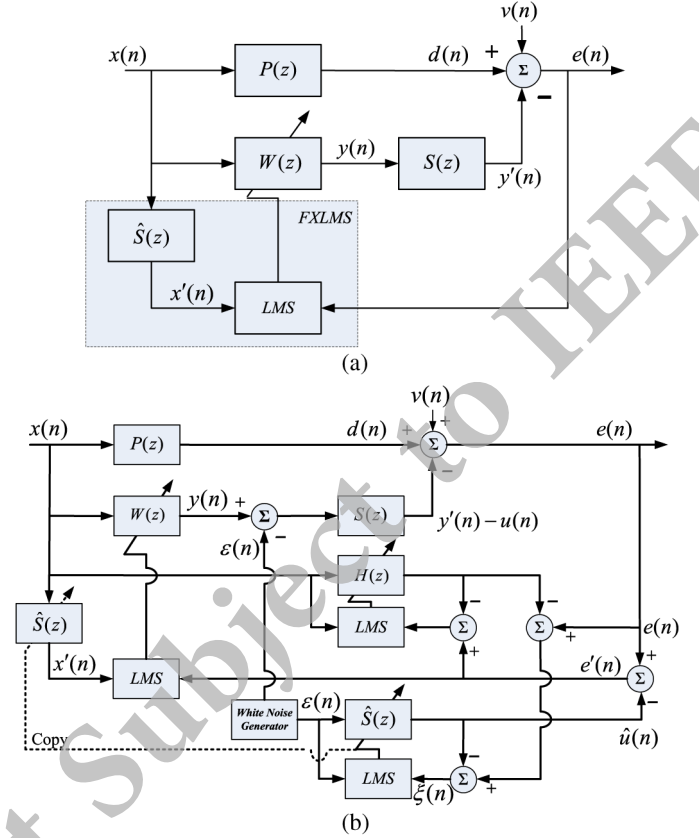


Fig. 1. Block diagram of an ANC system. (a) Basic structure. (b) Complete structure with online secondary path modeling.

microphone and the error microphone.  $W(z)$  is convolved with the loudspeaker system  $S(z)$  in the secondary path to cancel  $d(n)$ . The background noise  $v(n)$  is usually uncorrelated with  $x(n)$  and adds to the cancellation error signal  $e(n)$ . The objective of  $W(z)$  is to minimize the mean-square error (MSE) of  $e(n)$ . Denote the output of  $P(z)$  by  $d(n)$  and the impulse response of  $S(z)$  by  $s(n)$ . Let  $K$  be a sufficient tap length for  $W(z)$ , the coefficient vector  $W(z)$  at time instant  $n$  is  $\mathbf{w}_K(n) = [w_0(n)w_1(n)\cdots w_{K-1}(n)]^T$ , and the input noise vector  $\mathbf{x}_K(n) = [x(n)x(n-1)\cdots x(n-K+1)]^T$ . The cancellation error signal can be expressed as

$$e(n) = d(n) - [\mathbf{x}_K^T(n)\mathbf{w}_K(n)] * s(n) + v(n), \quad (1)$$

where  $*$  denotes linear convolution.

Let  $\hat{\zeta}(n) = e^2(n)$ . By minimizing the MSE, the LMS algorithm is to update  $\mathbf{w}_K(n)$  in the negative gradient direction of  $\hat{\zeta}(n)$  with a step size  $\mu$  by

$$\mathbf{w}_K(n+1) = \mathbf{w}_K(n) - \frac{\mu}{2} \nabla \hat{\zeta}(n), \quad (2)$$

where  $\nabla \hat{\zeta}(n)$  is an instantaneous estimate of the MSE gradient with  $\nabla \hat{\zeta}(n) = 2[\nabla e(n)]e(n)$ . From (1), we have  $\nabla e(n) = -s(n) * \mathbf{x}_K(n) = -\mathbf{x}'_K(n)$ , where  $\mathbf{x}'_K(n) = [x'(n)x'(n-1)\cdots x'(n-K+1)]^T$  with  $x'(n) = s(n) * x(n)$ . Therefore,  $\nabla \hat{\zeta}(n) = -2\mathbf{x}'_K(n)e(n)$ . Accordingly, the update equation of  $\mathbf{w}_K(n)$  becomes

$$\mathbf{w}_K(n+1) = \mathbf{w}_K(n) + \mu \mathbf{x}'_K(n)e(n). \quad (3)$$

Note, (3) includes  $S(z)$  in the update of the filter coefficients, which is conventionally called the *FxLMS algorithm*. Generally,  $S(z)$  is unknown, so it should be modeled by its estimated replica  $\hat{S}(z)$ , as shown in Fig. 1(a). In fact,

$$x'(n) = \hat{s}(n) * x(n), \quad (4)$$

where  $\hat{s}(n)$  is the impulse response of  $\hat{S}(z)$ .

### B. The Online Secondary Path Model

To obtain  $\hat{S}(z)$ , a complete ANC system usually includes an online secondary path estimation structure, for example, as depicted in Fig. 1(b) [28]. An internally generated zero-mean white noise  $\varepsilon(n)$  is added to the secondary path in order to estimate  $S(z)$ . However,  $\varepsilon(n)$  leads to an additional noisy component to  $e(n)$  as  $u(n) = \varepsilon(n) * s(n)$ , which will be canceled by  $\hat{u}(n)$  before forming a new error signal  $e'(n)$  to adjust the coefficients of  $W(z)$ . We have

$$e'(n) = d(n) - y'(n) + \xi(n) + v(n), \quad (5)$$

where  $\xi(n) = u(n) - \hat{u}(n)$  and  $\hat{u}(n) = \varepsilon(n) * \hat{s}(n)$ . To improve the convergence of  $\hat{S}(z)$ , an adaptive filter  $H(z)$  is introduced to cancel the residual difference between primary path and secondary path, i.e.,  $[p(n) - w(n) * s(n)] * x(n)$ . In this online modeling structure, the convergence of the FxLMS algorithm is affected by the residual auxiliary noise  $\xi(n) = [s(n) - \hat{s}(n)] * \varepsilon(n)$ .

Here,  $S(z)$  accounts for the composite effect of the loudspeaker, error microphone, and the circuits such as ADC, DAC, reconstruction filter, preamplifier, etc. At the initial stage, an advance measurement of  $S(z)$  can be used for  $\hat{S}(z)$  since  $S(z)$  is slowly time-varying due to the thermal noise and device aging [19], [22]. It is worthy to note, the delay of  $P(z)$  has to be longer than that of  $S(z)$ , or  $W(z)$  is unable to compensate  $S(z)$  for  $P(z)$  due to the limit of the causality constraint.

In a typical ANC system, the length of the impulse response of  $P(z)$  may be very long (hundreds, or moreover, thousands of taps), which directly affects the tap length of  $W(z)$ . As mentioned in [2], the maximum step size for the FxLMS algorithm is approximately

$$\mu_{\max} \approx \frac{1}{P_{x'}(K + \Delta)}, \quad (6)$$

where  $P_{x'}$  is the power of  $x'(n)$  and  $\Delta$  is the overall delay in the secondary path. When the tap length is long, the convergence rate will become very slow due to the limit of a very small step size. Therefore, a variable tap-length and step-size LMS algorithm is considered to remove this obstacle.

## III. THE VARIABLE TAP-LENGTH AND STEP-SIZE ANC METHOD

### A. The New FxLMS Algorithm

Denote the z-transform of  $\xi(n)$  by  $\Xi(z)$ . From (1) and (5), the z-transform of the new cancellation error signal  $e'(n)$  is

$$E'(z) = [P(z) - W(z)S(z)]X(z) + \Xi(z) + V(z). \quad (7)$$

When  $\Xi(z)$  and  $V(z)$  are small enough, a simple insight into (7) is that the cancellation error is close to zero, i.e.,  $E'(z) = 0$ , after the adaptive filter converges. Hence, we can see that  $W(z)$  is to realize the following transfer function:

$$W^o(z) = \frac{P(z)}{S(z)}. \quad (8)$$

In some circumstances, the decay envelopes of the impulse responses of  $P(z)$  and  $S(z)$  are presented on both sides of the maximum output response. For example,  $P(z)$  has an unsymmetric decay envelop for propagation delay while  $S(z)$  consists of a lowpass filter of symmetric coefficients for a linear-phase consideration. Therefore, we can generally treat that the impulse response of  $W(z)$  may have an unsymmetric decay envelop, in which  $M$  left taps and  $N$  right taps with respect to the maximum response are assumed here. Denote the left taps of the optimal coefficients by  $\mathbf{w}_L^o = [w_{-M}^o w_{-M+1}^o \cdots w_{-1}^o]^T$  and the right taps by  $\mathbf{w}_R^o = [w_0^o w_1^o \cdots w_{N-1}^o]^T$ , where  $w_0^o$  represents the maximum response. For simplicity, the following exponential functions are used to model the envelopes of the filter coefficients:

$$w_k^o = \begin{cases} e^{k\tau_L r_w(k)}, & k = -M, -M+1, \dots, -1 \\ e^{-k\tau_R r_w(k)}, & k = 0, 1, \dots, N-1, \end{cases} \quad (9)$$

where the decay factors  $\tau_L$  and  $\tau_R$  are positive constants, and  $r_w(k)$  is a zero-mean i.i.d. Gaussian random sequence with variance  $\sigma_{r_w}^2$ .

The proposed FxLMS algorithm adaptively adjusts its tap length and step size as time progresses. Denote by  $L(n)$ ,  $R(n)$ , and  $\mu(n)$  the left-hand side tap length, right-hand side tap length, and step size at time  $n$ , respectively. Suppose that  $L(n) \leq M$  and  $R(n) \leq N-1$ . Using the notations  $\mathbf{w}_{L(n),R(n)}(n)$  and  $\mathbf{x}'_{L(n),R(n)}(n)$  with subscripts  $L(n)$  and  $R(n)$  representing  $(L(n) + R(n))$ -tap filter vector and input vector, respectively, where  $\mathbf{w}_{L(n),R(n)}(n) = [w_{-L(n)}(n) \cdots w_{-1}(n)w_0(n)w_1(n) \cdots w_{R(n)-1}(n)]^T$  and  $\mathbf{x}'_{L(n),R(n)}(n) = [x'(n+L(n)) \cdots x'(n+1)x'(n)x'(n-1) \cdots x'(n-R(n)+1)]^T$ , we can rewrite (3) by replacing  $e(n)$  with  $e'(n)$  as

$$\mathbf{w}_{L(n+1),R(n+1)}(n+1) = \begin{bmatrix} \mathbf{0}_{L(n+1)-L(n)} \\ \mathbf{w}_{L(n),R(n)}(n) \\ \mathbf{0}_{R(n+1)-R(n)} \end{bmatrix} + \mathcal{M}(n+1) \times \mathbf{x}'_{L(n+1),R(n+1)}(n)e'(n). \quad (10)$$

where  $\mathbf{0}_j$  denotes the  $j \times 1$  zero vector and  $\mathcal{M}(n+1)$  is a diagonal matrix with

$$\mathcal{M}(n+1) = \begin{bmatrix} \mu_L(n+1)\mathbf{I}_{L(n+1)} & \mathbf{0}_{L(n+1) \times R(n+1)} \\ \mathbf{0}_{R(n+1) \times L(n+1)} & \mu_R(n+1)\mathbf{I}_{R(n+1)} \end{bmatrix}, \quad (11)$$

where  $\mu_L(n+1)$  and  $\mu_R(n+1)$  are generally considered as two different step sizes for  $\mathbf{w}_{L(n+1)}(n+1)$  and  $\mathbf{w}_{R(n+1)}(n+1)$ , respectively,  $\mathbf{I}_j$  is the  $j \times j$  identity matrix, and  $\mathbf{0}_{i \times j}$  denotes the  $i \times j$  zero matrix. If we consider the same step size,  $\mathcal{M}(n+1)$  actually becomes a scalar.

To express the vector  $\mathbf{w}_K(n)$  by the modeled part  $\mathbf{w}_{L(n),R(n)}(n)$ , we write  $\mathbf{w}_K(n) = [\mathbf{0}_{M-L(n)}^T \mathbf{w}_{L(n),R(n)}^T(n) \mathbf{0}_{N-R(n)}^T]^T$ . Now, split  $\mathbf{w}_K^o$

into three parts as  $\mathbf{w}_K^\circ = [\mathbf{w}_{M-L(n)}^{\circ T} \mathbf{w}_{L(n),R(n)}^{\circ T} \mathbf{w}_{N-R(n)}^{\circ T}]^T$ . The total coefficients error is

$$\mathbf{g}_K(n) = \mathbf{w}_K(n) - \mathbf{w}_K^\circ. \quad (12)$$

From (8), we can express the output of  $P(z)$  as

$$d(n) = [\mathbf{x}_K^T(n) \mathbf{w}_K^\circ] * s(n) \quad (13)$$

where  $\mathbf{x}_K(n) = [x(n-M) \cdots x(n-1)x(n)x(n+1) \cdots x(n+N-1)]^T$ . Substituting (13) into (1) and using (12), the cancellation error signal becomes

$$\begin{aligned} e'(n) &= [\mathbf{x}_K^T(n) \mathbf{w}_K^\circ - \mathbf{x}_{L(n),R(n)}^T(n) \mathbf{w}_{L(n),R(n)}(n)] \\ &\quad * s(n) + v'(n) \\ &= -[\mathbf{x}_K^T(n) \mathbf{g}_K(n)] * s(n) + v'(n) \\ &= -\mathbf{x}'_K^T(n) \mathbf{g}_K(n) + v'(n) \end{aligned} \quad (14)$$

where  $v'(n) = \xi(n) + v(n)$ . Substituting (14) for  $e'(n)$  in (10) and subtracting  $\mathbf{w}_K^\circ$  on both sides of (10), we obtain

$$\mathbf{g}_K(n+1) = \mathbf{A}(n) \mathbf{g}_K(n) + \mathcal{M}(n+1) \begin{bmatrix} \mathbf{0}_{M-L(n+1)} \\ \mathbf{x}'_{L(n+1),R(n+1)}(n) \\ \mathbf{0}_{N-R(n+1)} \end{bmatrix} \times v'(n), \quad (15)$$

where

$$\mathbf{A}(n) = \mathbf{I}_K - \mathcal{M}(n+1) \begin{bmatrix} \mathbf{0}_{M-L(n+1)} \\ \mathbf{x}'_{L(n+1),R(n+1)}(n) \\ \mathbf{0}_{N-R(n+1)} \end{bmatrix} \mathbf{x}'_K^T(n). \quad (16)$$

To develop the adaptation algorithm for  $L(n+1)$ ,  $R(n+1)$ , and  $\mu(n+1)$ , the MSD of  $\mathbf{g}_K(n)$  can be explored by

$$\Lambda(n) \equiv E[\|\mathbf{g}_K(n)\|_2^2], \quad (17)$$

where  $\|\cdot\|_2$  denotes  $\ell_2$  norm and  $E[\cdot]$  represents taking expectation. Assume that  $x(n)$  and  $v(n)$  are i.i.d. Gaussian sequences with variances  $\sigma_x^2$  and  $\sigma_v^2$ , respectively. According to the similar assumption and analysis in [26], we have

$$\Lambda(n+1) = \eta \Lambda(n) + (\beta - \eta) \Gamma(n+1) + \delta \Upsilon(n+1) + \gamma, \quad (18)$$

where

$$\Gamma(n+1) = E\left[\|\mathbf{w}_{M-L(n+1)}^\circ\|_2^2\right] + E\left[\|\mathbf{w}_{N-R(n+1)}^\circ\|_2^2\right] \quad (19)$$

$$\begin{aligned} \Upsilon(n+1) &= E\left[\|\mathbf{g}_{L(n+1)}(n+1)\|_2^2\right] \\ &\quad - E\left[\|\mathbf{g}_{R(n+1)}(n+1)\|_2^2\right] \end{aligned} \quad (20)$$

with

$$\mathbf{g}_{L(n+1)}(n+1) = \mathbf{w}_{L(n+1)}(n+1) - [\mathbf{w}_L^\circ]_{(-L(n+1):-1)},$$

$$\mathbf{g}_{R(n+1)}(n+1) = \mathbf{w}_{R(n+1)}(n+1) - [\mathbf{w}_R^\circ]_{(0:R(n+1)-1)},$$

and

$$\begin{aligned} \eta &= 1 - [\mu_L(n+1) + \mu_R(n+1)] \sigma_{x'}^2 + [L(n+1) \mu_L^2(n+1) \\ &\quad + R(n+1) \mu_R^2(n+1)] \sigma_{v'}^4, \end{aligned} \quad (21)$$

$$\beta = 1 + [L(n+1) \mu_L^2(n+1) + R(n+1) \mu_R^2(n+1)] \sigma_{x'}^4, \quad (22)$$

$$\delta = [\mu_R(n+1) - \mu_L(n+1)] \sigma_{x'}^2, \quad (23)$$

$$\gamma = [L(n+1) \mu_L^2(n+1) + R(n+1) \mu_R^2(n+1)] \sigma_{x'}^2 \sigma_{v'}^2, \quad (24)$$

and using (9) for  $\mathbf{w}_K^\circ$ , we have

$$E[\|\mathbf{w}_{M-L(n+1)}^\circ\|_2^2] = \frac{1 - e^{2[M-L(n+1)]\tau_L}}{1 - e^{2M\tau_L}} E[\|\mathbf{w}_M^\circ\|_2^2], \quad (25)$$

$$E[\|\mathbf{w}_{N-R(n+1)}^\circ\|_2^2] = \frac{e^{-2R(n+1)\tau_R} - e^{-2N\tau_R}}{1 - e^{-2N\tau_R}} E[\|\mathbf{w}_N^\circ\|_2^2], \quad (26)$$

where

$$E[\|\mathbf{w}_M^\circ\|_2^2] = \frac{e^{-2M\tau_L} (1 - e^{2M\tau_L})}{1 - e^{2\tau_L}} \sigma_{r_w}^2, \quad (27)$$

$$E[\|\mathbf{w}_N^\circ\|_2^2] = \frac{1 - e^{-2N\tau_R}}{1 - e^{-2\tau_R}} \sigma_{r_w}^2. \quad (28)$$

Note that the third term on the right-hand side of (18), i.e.,  $\delta \Upsilon(n+1)$ , is small compared with other terms. Hence, we will neglect it for simplicity in the following work.

The optimal tap lengths can be found by minimizing the MSD with respect to  $L(n+1)$  and  $R(n+1)$ . Let  $K(n+1) = L(n+1) + R(n+1)$ . Taking the derivatives of  $\Lambda(n+1)$  with respect to  $L(n+1)$  and  $R(n+1)$  and setting to zero, we have the following results after some mathematical manipulation:

$$L(n+1) = -\frac{1}{2\tau_L} \ln \frac{\mu_L^2(n+1)(1 - e^{2\tau_L})[\sigma_{x'}^2 \Lambda(n) + \sigma_{v'}^2]}{-2\tau_L [\mu_L(n+1) + \mu_R(n+1)] \sigma_{r_w}^2}, \quad (29)$$

and

$$R(n+1) = -\frac{1}{2\tau_R} \ln \frac{\mu_R^2(n+1)(1 - e^{-2\tau_R})[\sigma_{x'}^2 \Lambda(n) + \sigma_{v'}^2]}{2\tau_R [\mu_L(n+1) + \mu_R(n+1)] \sigma_{r_w}^2}. \quad (30)$$

Similarly, the optimal  $\mu_L(n+1)$  and  $\mu_R(n+1)$  can be found by taking the derivatives of  $\Lambda(n+1)$  with respect to  $\mu_L(n+1)$  and  $\mu_R(n+1)$  and setting to zero, respectively. Since  $\mu_L(n+1)$  and  $\mu_R(n+1)$  become related to  $L(n+1)$  and  $R(n+1)$ , respectively, it is a tough work to get the closed-form solution for the joint equations. Making the quasi-static assumptions  $L(n) \approx L(n+1)$  and  $R(n) \approx R(n+1)$ , a suboptimal solution can be efficiently found by replacing  $L(n+1)$  and  $R(n+1)$  by  $L(n)$  and  $R(n)$ , respectively, to calculate  $\mu_L(n+1)$  and  $\mu_R(n+1)$ . Finally, we have

$$\mu_L(n+1) = \frac{1 - \Gamma(n)/\Lambda(n)}{2L(n)[\sigma_{x'}^2 + \sigma_{v'}^2/\Lambda(n)]} \quad (31)$$

and

$$\mu_R(n+1) = \frac{1 - \Gamma(n)/\Lambda(n)}{2R(n)[\sigma_{x'}^2 + \sigma_{v'}^2/\Lambda(n)]}. \quad (32)$$

From (19), we can call  $\Gamma(n)$  the *unmodeled part's MSD* and  $\Lambda(n)$  the *total MSD*. Hence,  $\Gamma(n)/\Lambda(n) < 1$ . Also observed from (31) and (32), considering  $v'(n)$  is so small that it can be ignored and the adaptive filter approaches the perfect tap length, both  $\sigma_{v'}^2$  and  $\Gamma(n)$  approach zero such that  $\mu_L(n+1) \approx$

$\frac{1}{2L(n)\sigma_x^2}$  and  $\mu_R(n+1) \approx \frac{1}{2R(n)\sigma_x^2}$ , which are consistent with the convergence condition (6) excluding the effect of  $S(z)$  according to (8). If we consider using the same step size for  $L(n)$  and  $R(n)$ , i.e.,  $\mu_L(n) = \mu_R(n) = \mu(n)$ , then

$$\mu(n+1) = \frac{1 - \Gamma(n)/\Lambda(n)}{[K(n) + 2]\sigma_x^2 + [K(n)\sigma_v^2 - 2\sigma_x^2\Gamma(n)]/\Lambda(n)}. \quad (33)$$

In perfect convergence condition, we have  $\mu(n+1) \approx \frac{1}{(K+2)\sigma_x^2}$ .

### B. Recursive Form

To reduce the computational complexity in each recursion, a more useful scheme is to develop the recursive forms alternative to (29)–(33). Let us consider the general case for using two different step sizes in this discussion. The similar process can be easily adapted to the case for using the same step size. From (14), it can be shown that  $\sigma_e^2(n) = \sigma_x^2\Lambda(n) + \sigma_v^2$ . After re-manipulating (32), we have

$$\mu_L(n+1) = \frac{1}{2L(n)\Phi(n)}, \quad (34)$$

where

$$\Phi(n) = \frac{\sigma_e^2(n)}{\Lambda(n) - \Gamma(n)}. \quad (35)$$

Similarly, from (32) we have

$$\mu_R(n+1) = \frac{1}{2R(n)\Phi(n)}. \quad (36)$$

In fact, from (17) and (19) we can prove that

$$\Lambda(n) - \Gamma(n) = E[\|\mathbf{g}_{L(n)+R(n)}(n)\|_2^2], \quad (37)$$

which is the *modeled part's MSD*.

Now, let us move on writing the result of  $L(n+1) - L(n)$  and  $R(n+1) - R(n)$  based on (29) and (30). Note that  $\sigma_e^2(n)$  varies and essentially vanishes as time  $n$  progresses, and in consequence, the statistics of two successive samples can be viewed very close, i.e.,  $\sigma_e^2(n) = \sigma_e^2(n+1) = \sigma_e^2$ . Based on the above statement and some mathematical manipulation, we obtain the recursive forms for  $L(n+1)$  and  $R(n+1)$  as follows:

$$L(n+1) = L(n) + \frac{1}{2\tau_L} \ln \frac{\mu_L^2(n)[\mu_L(n+1) + \mu_R(n+1)]}{\mu_L^2(n+1)[\mu_L(n) + \mu_R(n)]}, \quad (38)$$

and

$$R(n+1) = R(n) + \frac{1}{2\tau_R} \ln \frac{\mu_R^2(n)[\mu_L(n+1) + \mu_R(n+1)]}{\mu_R^2(n+1)[\mu_L(n) + \mu_R(n)]}. \quad (39)$$

In practical use, the tap length is actually an integer number. Hence, we also need to round down  $L(n+1)$  and  $R(n+1)$  obtained from (38) and (39) to the nearest integers as the resultant.

### C. Convergence

The next question is whether the new FxLMS recursions can converge. Returning to (18), if we can prove that the second-order derivatives of  $\Lambda(n+1)$  with respect to  $L(n+1)$ ,  $R(n+1)$ ,  $\mu_L(n+1)$ , and  $\mu_R(n+1)$  are all positive, the MSD is a convex function of the above four variables and the developed recursions can find the minimum MSD. Taking the

second-order derivatives of (18) with respect to  $L(n+1)$  and  $R(n+1)$ ,  $\mu_L(n+1)$ , and  $\mu_R(n+1)$ , respectively, we have

$$\begin{aligned} \frac{\partial^2 \Lambda(n+1)}{\partial L^2(n+1)} &= -8\tau_L^2 \sigma_x^2 \sigma_v^2 [\mu_L(n+1) + \mu_R(n+1)] \\ &\quad \times \frac{-e^{-2L(n+1)\tau_L}}{1 - e^{-2\tau_L}}, \end{aligned} \quad (40)$$

$$\begin{aligned} \frac{\partial^2 \Lambda(n+1)}{\partial R^2(n+1)} &= 8\tau_R^2 \sigma_x^2 \sigma_v^2 [\mu_L(n+1) + \mu_R(n+1)] \\ &\quad \times \frac{e^{-2R(n+1)\tau_R}}{1 - e^{-2\tau_R}}, \end{aligned} \quad (41)$$

$$\frac{\partial^2 \Lambda(n+1)}{\partial \mu_L^2(n+1)} = 2L(n+1)\sigma_x^2 \sigma_e^2(n) + 2\sigma_x^4 [\Lambda(n) - \Gamma(n)], \quad (42)$$

and

$$\frac{\partial^2 \Lambda(n+1)}{\partial \mu_M^2(n+1)} = 2R(n+1)\sigma_x^2 \sigma_e^2(n) + 2\sigma_x^4 [\Lambda(n) - \Gamma(n)]. \quad (43)$$

In (40) and (41), since  $\tau_L > 0$  and  $\tau_R > 0$ ,  $1 - e^{-2\tau_L} < 0$  and  $1 - e^{-2\tau_R} > 0$ . In (42) and (43),  $\Lambda(n) - \Gamma(n) > 0$  based on (37). Therefore, (40)–(43) are all positive and then, we have shown that the total MSD is a convex function of  $L(n+1)$ ,  $R(n+1)$ ,  $\mu_L(n+1)$ , and  $\mu_R(n+1)$ . The new variable tap-length and step-size FxLMS algorithm can converge to the minimum MSD.

### D. Practical Issues for ANC Applications

In typical ANC applications, a proper tap length of  $W(z)$  is unknown a priori. Conventional ANC employing a fixed-tap-length FxLMS algorithm may lead to insufficient steady-state performance by using a small tap length while to slow convergence by using a large tap length. Hence, the variable-tap-length FxLMS algorithm is very suited to a realistic ANC system. The new algorithm gives a better tradeoff between the MSD performance and the convergence rate compared to the fixed-tap-length algorithm. Some practical issues about this new algorithm are addressed as follows.

1) *Delay of the Control Filter*: The purpose of the control filter  $W(z)$  is to compensate  $S(z)$  for canceling the reference noise  $x(n)$  passing through  $P(z)$ , in which  $S(z)$  inherently has delay brought by the realistic circuits and audio components. The propagation delay of  $P(z)$  depends on the circumstances in applications, however, it is required to be larger than that of  $S(z)$  or the ANC structure is not realizable as mentioned in [2]. In the proposed FxLMS algorithm,  $w_0^o(n)$  plays the role of the optimal delay position for  $W(z)$  to compensate for the delay difference between  $P(z)$  and  $S(z)$ . The determination of a proper delay for  $W(z)$  is required prior to employing the variable-tap-length FxLMS algorithm. An implementation method to find the optimal position of  $w_0^o(n)$  can be described as follows. First, we setup a sufficient length of buffer for  $W(z)$  depending on the application. A priori measure can help to find a proper initial delay position to assign  $w_0(n)$  in the buffer. Then, the proposed algorithm executes the growth of  $L(n+1)$  and  $R(n+1)$  through computing  $\Lambda(n+1)$  for the given delay position. The optimal position for  $w_0(n)$  can be obtained by a simple search for finding the minimum steady-state  $\Lambda(n+1)$  with changing the delay position over a range of nearby positions around the initial delay position. Actually, the search for the optimal delay

position is no more needed if  $P(z)$  and  $S(z)$  do not experience essential change.

2) *The Ideal Tap Lengths of the Control Filter:* In (9), we assume that  $M$  and  $N$  are the ideal tap lengths for  $\mathbf{w}_L^o$  and  $\mathbf{w}_R^o$ , respectively. They are involved in computing (19). In the proposed algorithm, choosing sufficiently large  $M$  and  $N$  such that  $e^{-M\tau_L}$  and  $e^{-N\tau_R}$  approach zero, for example, 0.01, we have  $M\tau_L = N\tau_R \approx 4.6$ . In general,  $\tau_L$  and  $\tau_R$  are quite small and we choose sufficiently large  $M$  and  $N$ , for example, at least,  $M = \lfloor \frac{4.6}{\tau_L} \rfloor$  and  $N = \lfloor \frac{4.6}{\tau_R} \rfloor$ , for practical applications, then  $1 - e^{-2\tau_L} \approx -2\tau_L$  and  $1 - e^{-2\tau_R} \approx 2\tau_R$ . In consequence, (19) can be approximated as

$$\Gamma(n+1) = \left( \frac{1}{2\tau_L} e^{-2L(n+1)\tau_L} + \frac{1}{2\tau_R} e^{-2R(n+1)\tau_R} \right) \sigma_{r_w}^2, \quad (44)$$

which is independent of  $M$  and  $N$ . That is, using larger  $M$  and  $N$  in the algorithm will not affect the MSD performance.

3) *Envelop Decay Factor:* The decay factors  $\tau_L$  and  $\tau_R$  are necessary information prior to performing the algorithm. When the circumstance of the application is stationary,  $\tau_L$  and  $\tau_R$  can be roughly measured in advance. The following method can be used for online modification of the factors  $\tau_L$  and  $\tau_R$ . For example, the least-squares method for the estimate of  $\tau_R$  at time  $n+1$  is

$$\hat{\tau}_R(n+1) = \arg \min_{\tau} \sum_{i=1}^N [e^{-i\tau} - \hat{w}_{R,i}(n)]^2 \quad (45)$$

where  $\hat{w}_{R,i}(n)$  is the  $i$ th element of  $\hat{\mathbf{w}}_R(n)$ . To solve (45) is a complicated and nonlinear problem. Alternatively, taking the log function of  $\hat{w}_{R,i}(n)$  is a simple while effective method,

$$\hat{\tau}_R(n+1) = \arg \min_{\tau} \sum_{i \in \Omega_s} [i\tau + \ln(\hat{w}_{R,i}(n))]^2, \quad (46)$$

where  $\Omega_s$  denotes the set of the elements in  $\hat{\mathbf{w}}_R(n)$  to be used for estimation. Finally, we have

$$\hat{\tau}_R(n+1) = \frac{\sum_{i \in \Omega_s} i \cdot [\ln(\hat{w}_{R,i}(n))]^2}{\sum_{i \in \Omega_s} i^2}. \quad (47)$$

The similar method can be applied to the estimate of  $\tau_L$ .

4) *Termination of the Tap-Length Growth:* In the variable-tap-length algorithm, we assume that  $L(n) \leq M$  and  $R(n) \leq N-1$ . However, in practical applications,  $M$  and  $N$  are unknown and possibly, there are no exact values due to the interference of the background noise. That is, the tap lengths can continue growing if no limit is imposed based on some criterion. The step size will, therefore, becomes too small to yield a satisfying MSD performance in a reasonable number of iterations because of an excess tap length. A simple method is to check the last  $Q$  new taps whether their total energy is effective, and terminate the growth of the tap length if the energy is below some threshold. Define that

$$T_L(n) = \sum_{j=0}^{Q-1} w_{-L(n)+j}^2(n) \quad (48)$$

and

$$T_R(n) = \sum_{j=0}^{Q-1} w_{R(n)-1-j}^2(n). \quad (49)$$

The growth termination conditions for  $L(n+1)$  and  $R(n+1)$  can be given by

$$T_L(n) \leq \kappa_L \text{ and } T_R(n) \leq \kappa_R \quad (50)$$

respectively, where  $\kappa_L$  and  $\kappa_R$  are the predefined thresholds.

### E. Algorithm Summary and Complexity Discussion

In Table I, we summarize the proposed FxLMS algorithm, provided with the numbers of additions and multiplications that are required to compute the variables in recursion. The main part in the FxLMS algorithms is to adaptively calculate the coefficients of the control filter. For the conventional method in (3), a predetermined tap length, say  $K$ , leads to  $K$  additions and  $2K$  multiplications, which are the minimum requirements of computational complexity for the conventional FxLMS method because the extra calculation for a variable step size  $\mu$  is possibly needed. However,  $K$  is usually chosen large enough to account for different situations. Also as listed in Table I, the proposed two step-size FxLMS algorithm requires  $K(n)+11$  additions/subtractions and  $2K(n)+29$  multiplications/divisions in total. There are also four exponential or logarithmic operations required to compute recursive variables. Here, we do not repeatedly count the operational numbers of the equations if they have the same computational terms, and the fixed values in recursion are treated as preprocessed results such as those in (27) and (28).

In addition to avoiding an over-tap-length of control filter, the new algorithm reduces the computational complexity required at the start-up of the ANC system. For the conventional method, the tap length is always fixed as  $K$  and actually the performance does not benefit from a longer tap length even with an excess cost. The numbers of additions and multiplications of the proposed algorithm are proportional to the growing tap lengths  $L(n)$  and  $R(n)$ , and thus, a lower computational complexity is required at the start-up. Since the multiplication is more complicated than the addition, the number of multiplications dominates the evaluation of the computational complexity. From Table I, the number of multiplications of the conventional FxLMS method is larger than that of the proposed algorithm as  $K > K(n) + 14$ .

## IV. SIMULATION RESULTS

Some numerical experiments have been conducted to validate the proposed variable-tap-length FxLMS algorithm equipped with different variable step sizes. In this section, simulation results for three different cases are provided to show the properties of convergence rate and steady-state performance of the proposed algorithm in comparison with some fixed-tap-length FxLMS algorithms. In Case 1, we verify the proposed algorithm to compare the MSD performance for different algorithms with a given  $W^o(z)$  that is generated from a zero-mean white Gaussian process  $r_w(k)$ . Then, we generate  $P(z)$  by  $P(z) = W^o(z)S(z)$ . In this case,  $W^o(z)$  exactly matches the assumption of the proposed algorithm. Once the estimate of  $W(z)$  is obtained as  $\hat{W}(z)$ , the MSD is evaluated through a 100 runs Monte Carlo simulation in decibels (dB) by calculating  $\|\hat{\mathbf{w}}(n) - \mathbf{w}_K^o(n)\|_2^2$  for each iteration. In Case 2, the  $P(z)$  and  $S(z)$  models are similar to the data taken from the disk included in [2]. The tap lengths of  $P(z)$  and  $S(z)$  are quite short compared to those used in Case 1. In Case 3, the

TABLE I  
THE SUMMARY OF THE PROPOSED FxLMS ALGORITHM AND COMPUTATIONAL COMPLEXITY

	Equations for FxLMS	add./sub.	mul./div.
Conventional FxLMS			
	$\mathbf{w}_K(n+1) = \mathbf{w}_K(n) + \mu \mathbf{x}'_K(n) e'(n)$	$K$	$2K$
Proposed FxLMS			
Initialization:			
	Environmental parameters: $\sigma_{x'}^2, \sigma_{v'}^2, \sigma_{r_w}^2, \tau_L, \tau_R$		
	Algorithmic initials: $L(0), R(0), \Gamma(0), \Lambda(0), \mathbf{w}_{L(n), R(n)}(0)$		
	Time index: $n = 0$		
Loop:			
	$\sigma_{e'}^2(n) = \sigma_{x'}^2 \Lambda(n) + \sigma_{v'}^2$	1	1
	$\mu_L(n+1) = \frac{\Lambda(n) - \Gamma(n)}{2L(n)\sigma_{e'}^2(n)}$	1	3
	$\mu_R(n+1) = \frac{\mu_L(n+1)L(n)}{R(n)}$	0	2
	$L(n+1) = -\frac{1}{2\tau_L} \ln \frac{\mu_L^2(n+1)(1-e^{-2\tau_L})\sigma_{e'}^2(n)}{-2\tau_L[\mu_L(n+1)+\mu_R(n+1)]\sigma_{r_w}^2}$	1	6
	$R(n+1) = -\frac{1}{2\tau_R} \ln \frac{\mu_R^2(n+1)(1-e^{-2\tau_R})\sigma_{e'}^2(n)}{2\tau_R[\mu_L(n+1)+\mu_R(n+1)]\sigma_{r_w}^2}$	0	4
	$E[\ \mathbf{w}_{M-L(n+1)}^\circ\ _2^2] = \frac{e^{-2M\tau_L} - e^{-2L(n+1)\tau_L}}{1 - e^{-2\tau_L}} \sigma_{r_w}^2$	1	2
	$E[\ \mathbf{w}_{N-R(n+1)}^\circ\ _2^2] = \frac{e^{-2R(n+1)\tau_R} - e^{-2N\tau_R}}{1 - e^{-2\tau_R}} \sigma_{r_w}^2$	1	2
	$\Gamma(n+1) = E[\ \mathbf{w}_{M-L(n+1)}^\circ\ _2^2] + E[\ \mathbf{w}_{N-R(n+1)}^\circ\ _2^2]$	1	0
	$\beta = 1 + [L(n+1)\mu_L^2(n+1) + R(n+1)\mu_R^2(n+1)]\sigma_{x'}^4$	2	5
	$\eta = \beta - [\mu_L(n+1) + \mu_R(n+1)]\sigma_{x'}^2$	1	1
	$\gamma = [L(n+1)\mu_L^2(n+1) + R(n+1)\mu_R^2(n+1)]\sigma_{x'}^2\sigma_{v'}^2$	0	1
	$\Lambda(n+1) = \eta\Lambda(n) + (\beta - \eta)\Gamma(n+1) + \gamma$	2	2
	$\mathcal{M}(n+1) = \begin{bmatrix} \mu_L(n+1)\mathbf{I}_{L(n+1)} & \mathbf{0}_{L(n+1) \times R(n+1)} \\ \mathbf{0}_{R(n+1) \times L(n+1)} & \mu_R(n+1)\mathbf{I}_{R(n+1)} \end{bmatrix}$	0	0
	$\mathbf{w}_{L(n+1), R(n+1)}(n+1) = \begin{bmatrix} \mathbf{0}_{L(n+1)-L(n)} \\ \mathbf{w}_{L(n), R(n)}(n) \\ \mathbf{0}_{R(n+1)-R(n)} \end{bmatrix} + \mathcal{M}(n+1)\mathbf{x}'_{L(n+1), R(n+1)}(n)e'(n)$	$K(n)$	$2K(n)$
	Increase time index $n := n+1$ and go back to Loop.		

Note: Four exp or log operations are also required for the proposed FxLMS algorithm to compute recursive variables.

TABLE II  
SIMULATION SETUP FOR THE THREE CASES

Parameters	Case 1	Case 2	Case 3
length of $P(z)$	1088	145	261
length of $S(z)$	65	51	51
$K$	1024	95 <sup>†</sup>	211 <sup>†</sup>
$\sigma_{r_w}^2$	0.01	0.01	0.01
$(\tau_L, \tau_R)$	(0.01, 0.005)	(0.009, 0.006)	(0.03, 0.02)
$(\sigma_x^2, \sigma_\varepsilon^2, \sigma_v^2)$	(1, 1, 0.01)	(1, 1, 0.01)	(1, 1, 0.01)
$Q$	20	10	10
$(\kappa_L, \kappa_R)$	(0.01, 0.001)	(0.1, 0.001)	(0.01, 0.001)

<sup>†</sup> is assumed for FTL algorithms.

magnitude response of  $P(z)$  are worse than that of  $P(z)$  used in Case 2, and has a longer tap length. We use the same  $S(z)$  in Case 2 and Case 3. The simulation parameters for the three cases are summarized in Table II. Since  $W^\circ(z)$  is unknown in Case 2 and Case 3, only the noise reduction performance is evaluated instead of the MSD. We define the noise reduction ratio  $NRR$  (dB) as

$$NRR \text{ (dB)} = 10 \log_{10} \left( \frac{E[d^2(n)]}{E[e'^2(n)]} \right), \quad (51)$$

where  $E[\cdot]$  is then approximated by ensemble average in our simulations for simplicity. In all cases,  $\hat{S}(z)$  is obtained with online estimation in the structure as depicted in Fig. 1(b). The

impulse responses and frequency responses of  $P(z)$  and  $S(z)$  for the three cases are plotted in Figs. 2–6.

Some fixed-tap-length algorithms are compared with the proposed algorithm for different step sizes. Except for Case 1, the optimal tap length for the fixed-tap-length algorithms is actually unknown. For the purpose of comparison, the tap length obtained from the steady-state tap length of the proposed algorithm is used for the fixed-tap-length algorithms. For simplifying the figure legend, we abbreviate the fixed-tap-length algorithms as FTL and the variable-tap-length algorithms as VTL. The algorithms for comparison are briefly described as follows:

- FTL–LS: A large step size for maintaining the FxLMS stability can be set as  $\mu_{\max} = \frac{1}{(K+2)\sigma_{x'}^2}$ , according to the description below (33).
- FTL–SS: A smaller step size for the FxLMS algorithm will provide a steady-state performance better close to the proposed algorithm than a large step size. In order to reach the steady-state performance within the inspected iteration number, we set  $\mu_{\min} = 0.2\mu_{\max}$ .
- FTL–NSS: The normalized LMS algorithm uses a normalized step size (NSS) to optimize the speed of convergence while maintaining a satisfying steady-state performance [2]. The step size to be used here is

$$\mu(n) = \frac{\alpha}{\mathbf{x}'_K^T(n)\mathbf{x}'_K(n)}, \quad (52)$$

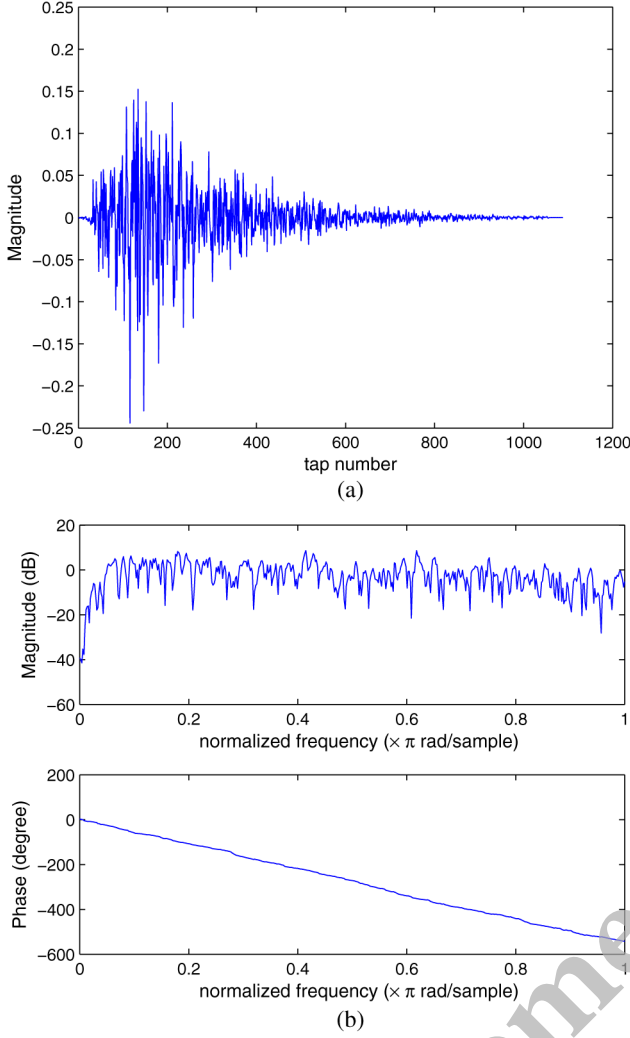


Fig. 2. Impulse response and frequency response of  $P(z)$  in Case 1. (a) Impulse response of  $P(z)$ . (b) Frequency response of  $P(z)$ .

where the normalizing factor  $\alpha$  is generally chosen with the range  $0 < \alpha < 2$ . In our simulations, we set  $\alpha = 0.4$ .

- FTL-VSS: A variable step size (VSS) scheme for the FxLMS algorithm, similar to [12], is simulated using

$$\mu(n) = \rho(n)\mu_{\max} + [1 - \rho(n)]\mu_{\min} \quad (53)$$

where  $\rho(n)$  is a weighting factor,  $0 \leq \rho(n) \leq 1$ , and is calculated by  $\rho(n) = \frac{P_e(n) - P_{e,\min}}{P_{e,\max} - P_{e,\min}}$  with  $P_{e,\max}$  and  $P_{e,\min}$  representing the maximum and minimum average powers of  $e(n)$ , respectively and  $P_e(n) = \frac{1}{T} \sum_{i=n-T+1}^n e^2(n)$ , where  $T$  is an averaging constant with  $T = 200$  here.  $P_{e,\max}$  uses the average of the first 100 iterations of  $P_e(n)$  multiplied by 1.3 while  $P_{e,\min}$  uses the average of the last 100 iterations of  $P_e(n)$  multiplied by 0.7.

- VTL-VSS-I: The proposed variable-tap-length algorithm with a universal step size  $\mu(n)$ .
- VTL-VSS-II: The proposed variable-tap-length algorithm with two different step sizes  $\mu_L(n)$  and  $\mu_R(n)$ .
- VTL-VSS-III: This scheme uses the proposed variable-tap-length algorithm, but with a simplified variable step size. From [27], we use the estimated tap length  $K(n)$  for

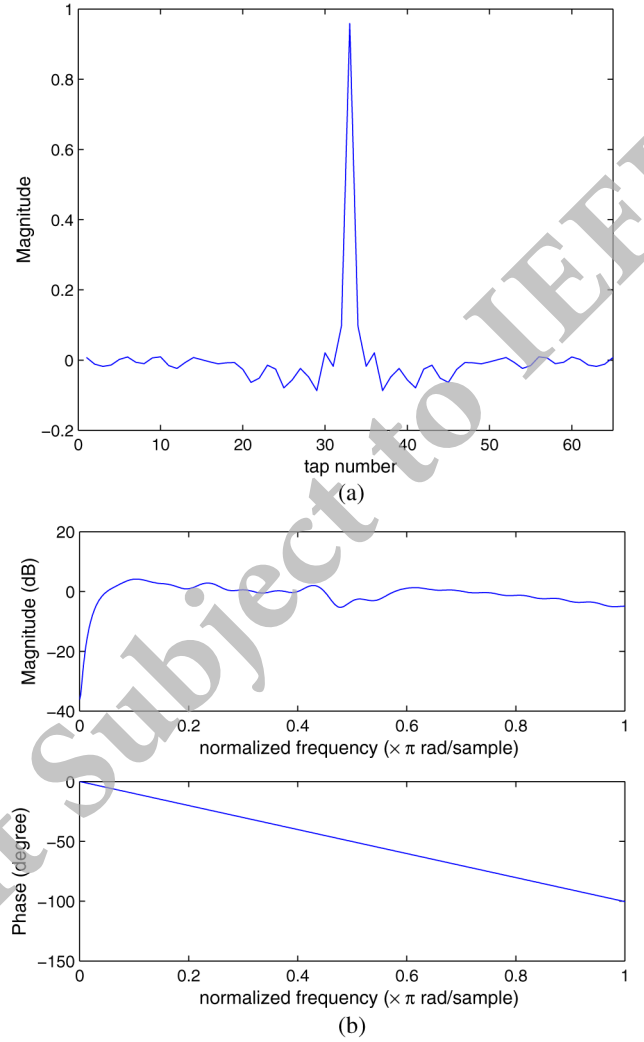


Fig. 3. Impulse response and frequency response of  $S(z)$  in Case 1. (a) Impulse response of  $S(z)$ . (b) Frequency response of  $S(z)$ .

each iteration to replace the maximum tap length  $K$  in (6). Then, we have variable step sizes for VTL with

$$\mu_L(n) = \frac{0.5}{(L(n) + \delta)\sigma_x^2}, \quad (54)$$

and

$$\mu_R(n) = \frac{0.5}{(R(n) + \delta)\sigma_x^2}, \quad (55)$$

where  $\delta$  is a factor related to the delay of the secondary path, and assuming  $\delta$  is known a priori in simulations.

#### A. Case 1

The tap length of  $W^o(z)$  is  $K = 1024$ , which is divided into  $M = 124$  and  $N = 900$ . The tap length of the loudspeaker model  $S(z)$  is  $L = 65$ , so that of  $P(z)$  is 1088. The variance of the Gaussian process for  $\mathbf{w}_K^o(n)$  is  $\sigma_{r_w}^2 = 0.01$ . The exponential decay factors are  $\tau_L = 0.01$  and  $\tau_R = 0.005$ . The primary noise  $x(n)$ , auxiliary noise  $\varepsilon(n)$ , and background noise  $v(n)$  are zero-mean i.i.d. and uncorrelated Gaussian processes with variances  $\sigma_x^2 = 1$ ,  $\sigma_\varepsilon^2 = 1$ , and  $\sigma_v^2 = 0.01$ , respectively. By terminating

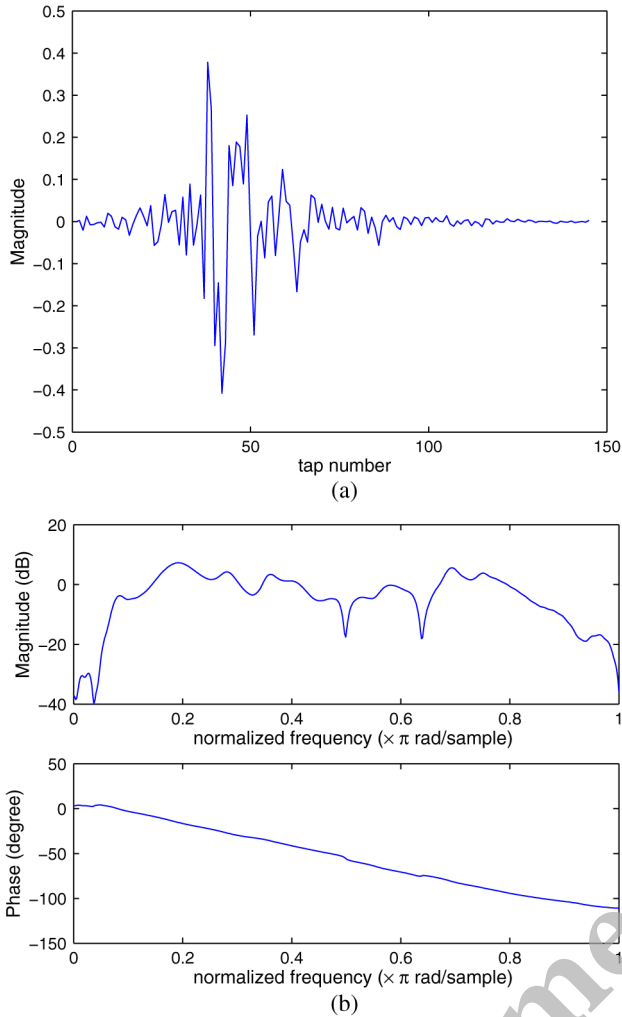


Fig. 4. Impulse response and frequency response of  $P(z)$  in Case 2. (a) Impulse response of  $P(z)$ . (b) Frequency response of  $P(z)$ .

the growth of the tap lengths for the proposed algorithm, we set  $Q = 20$ ,  $\kappa_L = 0.01$  and  $\kappa_R = 0.0001$ .

From Fig. 7, we find that the VTL algorithms generally have faster convergence and better performance than the FTL algorithms. For FTL algorithms, FTL-LS has relatively faster convergence rate because of a larger step size, however, it leads to the worst steady-state MSD performance, which is similar to the FTL-NS algorithm. FTL-VSS takes the advantages of FTL-SS and FTL-LS for a step size that is compromised to dramatically improve the steady-state performance better than FTL-LS, also with better convergence rate than FTL-SS. For VTL algorithms, the proposed VTL-VSS-I has the fastest convergence rate while the proposed VTL-VSS-II reaches the best performance. Although the convergence speed of VTL-VSS-III is similar to that of VTL-VSS-I, its step size is too simple to provide a better steady-state performance than the proposed step sizes. In addition to either slower convergence or worse performance, another disadvantages of the FTL algorithms is to set a proper tap length a priori, which is a problem in practical environments, especially when the device is aging. The convergence curves of tap lengths and step sizes of the FTL algorithms are shown in Fig. 8(a) and (b). It is worth to note, although FTL-VSS-II provides a better flexibility of two different step sizes to reach

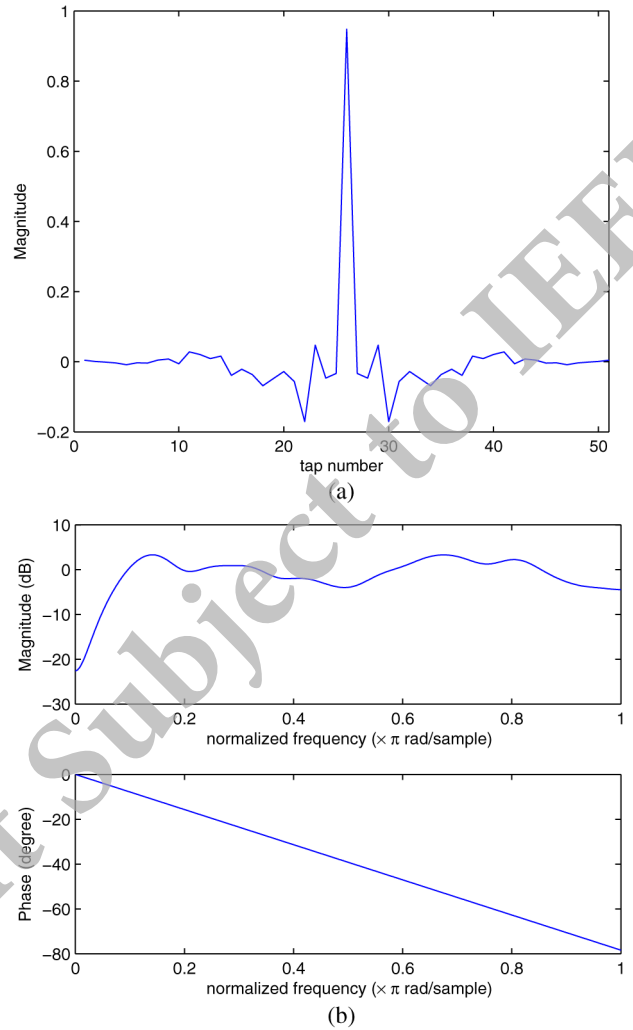


Fig. 5. Impulse response and frequency response of  $S(z)$  in Case 2 and Case 3. (a) Impulse response of  $S(z)$ . (b) Frequency response of  $S(z)$ .

the steady-state tap lengths very soon, the MSD convergence rate may not benefit from this due to getting a smaller step size early, in spite of achieving a superior MSD performance at last.

The steady-state  $W(z)$  in this case is shown in Fig. 9(a), where the blue line is the optimum coefficients while the red line is the estimated coefficients obtained by the proposed VTL-VSS-II algorithm. The resultant  $W(z)$  after 50000 iterations has 1021 taps. Since the steady-state MSD is as low as about -22 dB, there is almost no significant difference between the optimum coefficients and the estimated ones. Moreover, our simulation takes into account the background noise at -20 dB in this case, so the absolute difference level after about 400 taps seems similar as shown in Fig. 9(b) because the coefficients after 400 taps may be so small that do not have distinct influence on the resulted output signal in presence of -20 dB background noise. That is, the estimation accuracy for small coefficients (possibly after 400 taps in this case) is disturbed by the background noise. No doubt, the MSD and the absolute difference level for small coefficients will become smaller if we set lower background noise.

In Fig. 10, we show the relationship between steady-state  $\Lambda(n)$  and the secondary path delay from -20 shifted taps through

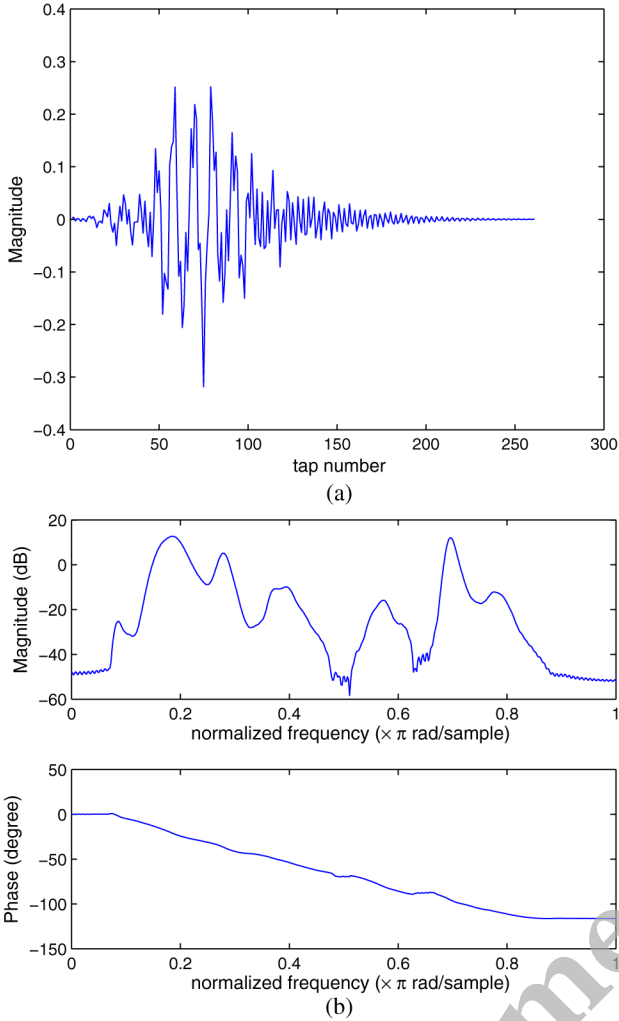


Fig. 6. Impulse response and frequency response of  $P(z)$  in Case 3. (a) Impulse response of  $P(z)$ . (b) Frequency response of  $P(z)$ .

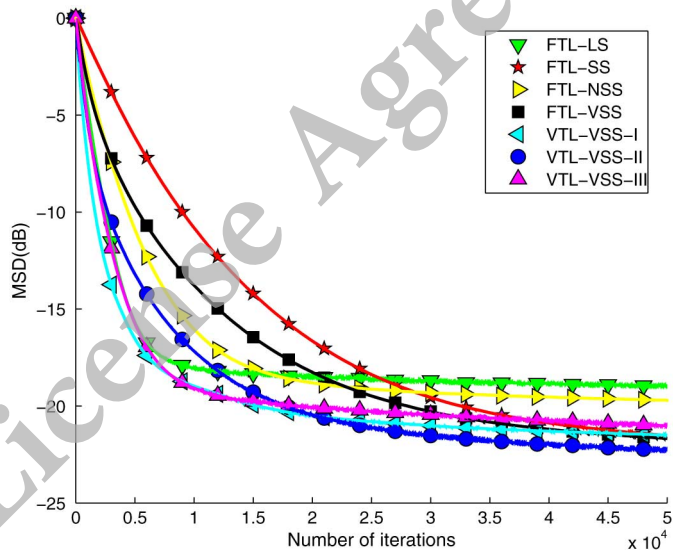


Fig. 7. Comparison of the MSD performance for different ANC algorithms in Case 1.

20 shifted taps with respect to the maximum response output. The best performance of steady-state  $\Lambda(n)$  is at zero delay shift and the performance degrades as the number of the delay shift

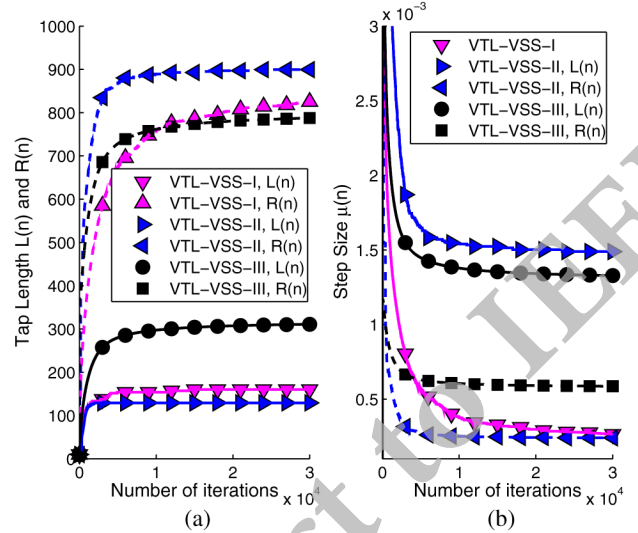


Fig. 8. Convergence of the tap lengths and step sizes for the proposed variable-tap-length algorithm in Case 1. (a) Tap lengths. (b) Step sizes.

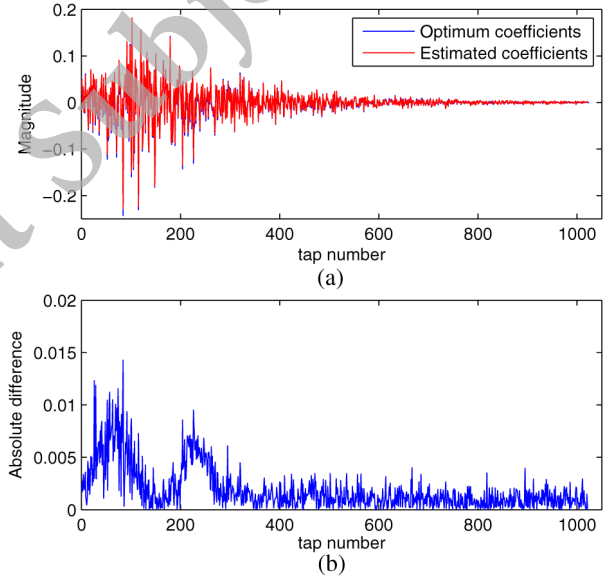


Fig. 9. Steady-state control filter coefficients in Case 1. (a) Optimum coefficients (blue) and estimated coefficients (red). (b) The absolute difference.

taps increases. Note that this curve is not symmetric because the impulse response of  $P(z)$  has different exponential decay factors. From this curve, the optimum secondary delay position for  $w_0^o(n)$  can be found by searching for the delay tap of the minimum steady-state  $\Lambda(n)$ .

An experiment is employed to see the effect of primary noise reduction for VTL-VSS-II. Suppose the input noise  $x(n)$  is exacerbated with variances  $\sigma_x^2 = 9, 49, 100$ , and returned to unity at the 15000th, 25000th, 35000th, and 45000th iterations, respectively, as shown in Fig. 11(a). From Fig. 11(b), the ANC output maintains its cancellation error noise  $e'(n)$  without significant change compared to the original output level for noise control. To evaluate the noise reduction performance of the ANC, Fig. 12 plots the  $NRR$  comparison of the VTL algorithms and the FTL algorithms. The cancellation error noise  $e'(n)$  is suppressed to about 1/10 of the original input noise  $x(n)$  with about 20 dB  $NRR$ , which can be also observed

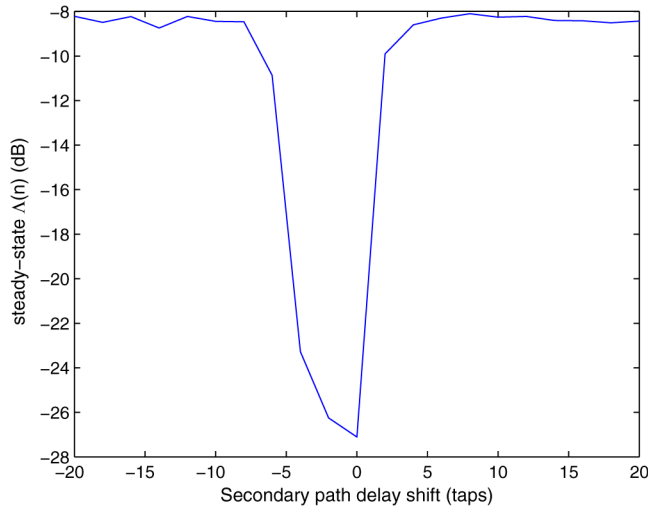


Fig. 10. MSD v.s. the secondary path delay shifts with respect to the maximum response output in Case 1.

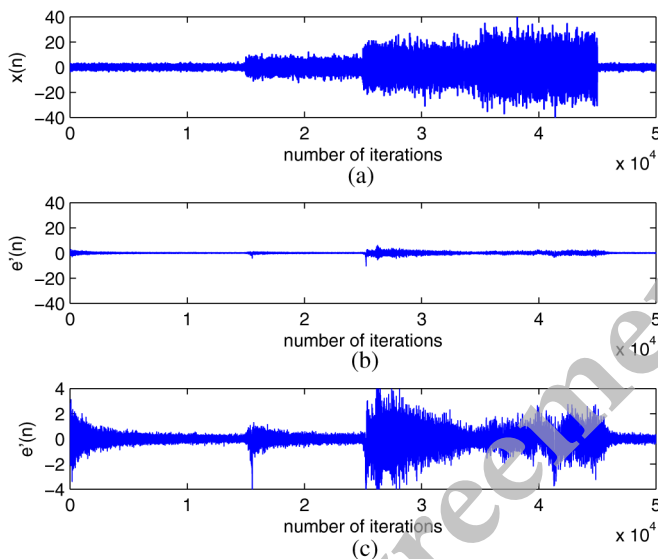


Fig. 11. The effect of noise reduction in Case 1. (a) Primary noise  $x(n)$ . (b) Cancellation error signal  $e'(n)$ . (c) The magnified magnitude scale of (b).

by comparing Figs. 11(a) and (c). In addition to a better MSD performance, the proposed algorithm has superior convergence rate and steady-state performance in  $NRR$ .

To check the robustness of the proposed algorithms, we consider the situation that the response of the electro-acoustic plant abruptly changes during the ANC adaptation process. Our simulation setup is all the same as the above in Case 1, except for using a shortened impulse response of  $P(z)$  before the 28000th iteration. The shortened plant is generated from the impulse response of  $P(z)$  multiplied by  $e^{(n-100)/15}$ ,  $n = 1, 2, \dots, 100$ , for the first 100 taps and by  $e^{(101-n)/350}$ ,  $n = 101, 102, \dots, 1024$ , for the last 924 taps, and then the new impulse response is normalized. In Fig. 13, the MSD performance significantly degrades at the iteration number of changing the  $P(z)$  response. However, all of the different ANC algorithms can converge as the previous results, in where the proposed algorithms are not deteriorated and still have superior convergence rate and performance. As shown in

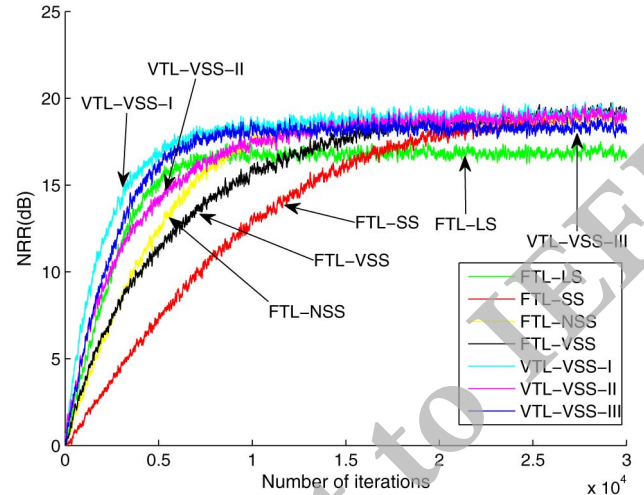


Fig. 12. Comparison of  $NRR$  performance for different ANC algorithms in Case 1.

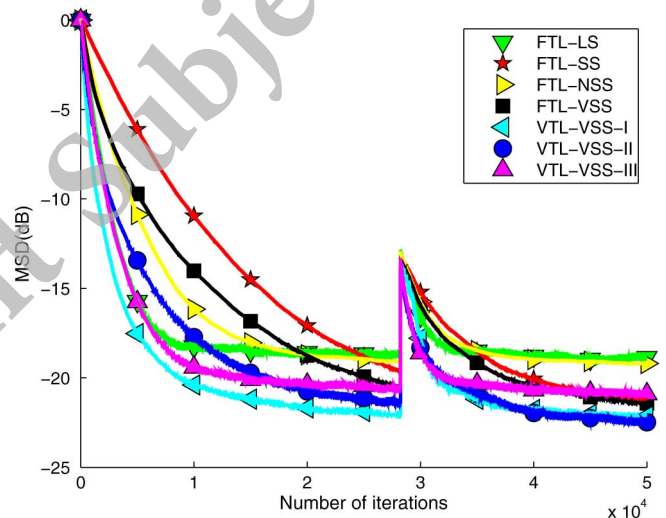


Fig. 13. Comparison of the MSD performance with abrupt response change of  $P(z)$  in Case 1.

Fig. 14(a), VTL-VSS-I and VTL-VSS-II increase their numbers of taps after the response changes. Actually, the change of the response causes the change of step sizes as shown in Fig. 14(b), and then leads to the increase of tap lengths. In contrast, VTL-VSS-III almost does not change its tap length and step size in this case because of using a simple equation to calculate the step size.

### B. Case 2

In this case, the tap length of  $P(z)$  is 145 and that of the loudspeaker system model  $S(z)$  is  $L = 51$ . The statistics of primary noise, auxiliary noise, and background noise are the same as those used in Case 1. For the FTL algorithms, we assume the tap length of  $W^o(z)$  is  $K = 95$ . The initial exponential decay factors used for the VTL algorithms are  $\tau_L = 0.009$  and  $\tau_R = 0.006$ . The parameter  $\sigma_{r_w}^2$  of the Gaussian process for  $\mathbf{w}_K^o(n)$  is set to be 0.01. To terminate the growth of the tap lengths for the proposed algorithms, we choose  $Q = 10$ ,  $\kappa_L = 0.1$ , and  $\kappa_R = 0.0001$ , where we set a smaller  $Q$  than

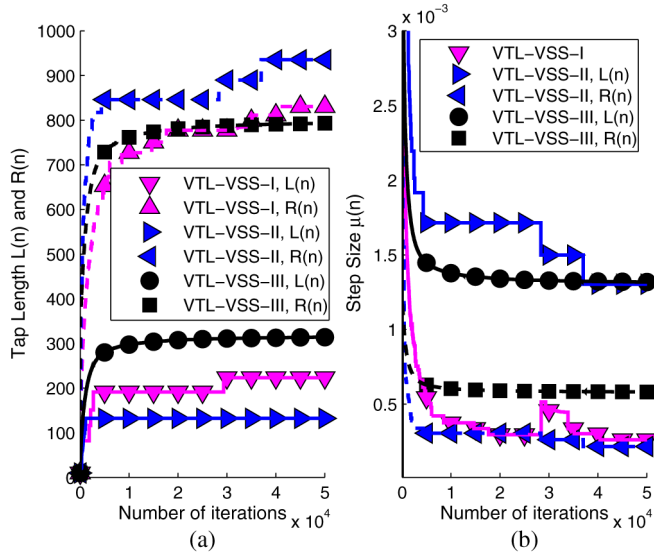


Fig. 14. Convergence of the tap lengths and step sizes with abrupt response change of  $P(z)$  in Case 1. (a) Tap lengths. (b) Step sizes.

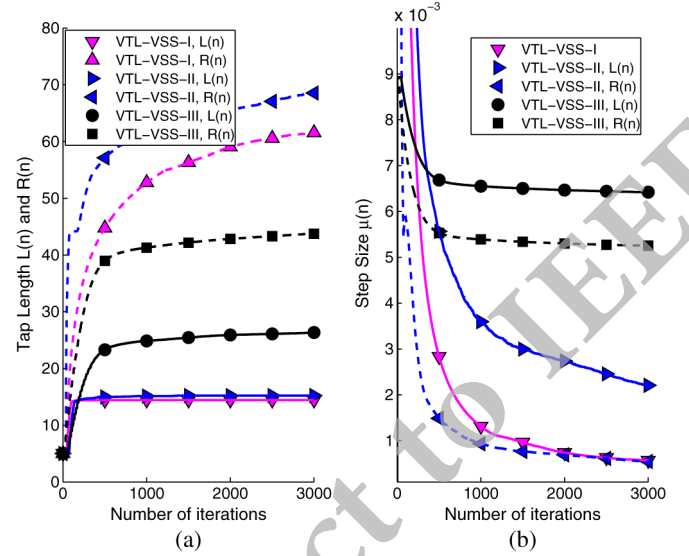


Fig. 16. Convergence of the tap lengths and step sizes for the proposed variable-tap-length algorithm in Case 2. (a) Tap lengths. (b) Step sizes.

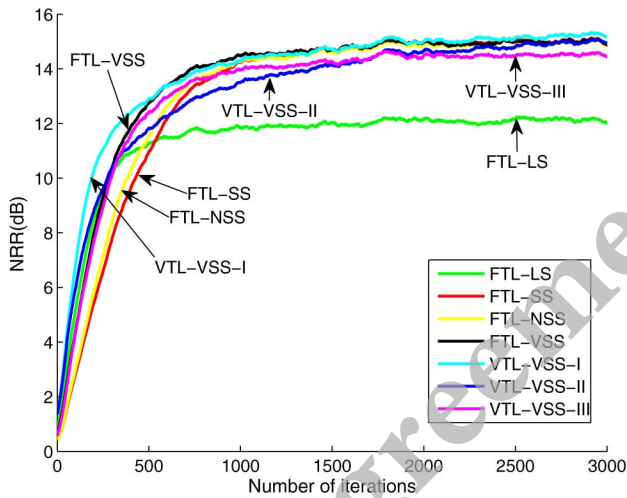


Fig. 15. Comparison of  $NRR$  performance for different ANC algorithms in Case 2.

that used in Case 1 because the tap lengths in this case are relatively shorter than those in Case 1.

For a case of short tap lengths, the difference of the convergence speed in  $NRR$  between the FTL algorithms and the VTL algorithms becomes not very distinct, as shown in Fig. 15. However, it is worth to note that we simulate the FTL algorithms based on the assumption of knowing the ideal tap length of  $W^o(z)$ , which is actually unknown in practical situations. Even with the ideal simulation condition for the FTL algorithms, the VTL algorithms still have comparable convergence speed and steady-state performance. From Fig. 16, we can see that VTL-VSS-II reaches a better ideal tap length for  $W(z)$  with about 88 taps while VTL-VSS-I with about 78 taps. The VTL-VSS-III algorithm gives a shorter tap length for  $L(n)$  and a longer tap length for  $R(n)$ , and shows a worse  $NRR$  performance even though its convergence speed is a little faster than VTL-VSS-II.

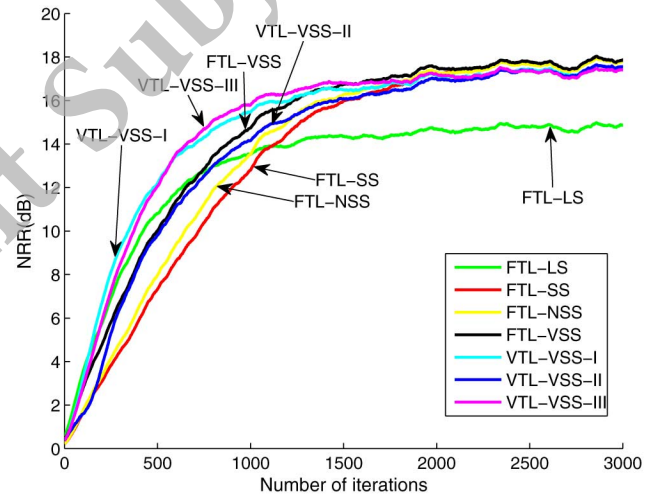


Fig. 17. Comparison of  $NRR$  performance for different ANC algorithms in Case 3.

### C. Case 3

The tap length of  $P(z)$  is 261 and that of  $S(z)$  is  $L = 51$ , where the frequency response of  $P(z)$  is worse than the former with a longer tap length. The statistics of primary noise, auxiliary noise, and background noise are also the same as those used in Case 1. For the FTL algorithms, we assume the tap length of  $W^o(z)$  is  $K = 211$ . The initial exponential decay factors used for the VTL algorithms are  $\tau_L = 0.03$  and  $\tau_R = 0.02$ . The variance  $\sigma_{r_w}^2$  of the Gaussian process for  $w_K^o(n)$  is assumed to be 0.01. To terminate the growth of the tap lengths for the proposed algorithm, we set  $Q = 10$ ,  $\kappa_L = 0.01$  and  $\kappa_R = 0.0001$ .

Since the tap length of  $P(z)$  is a little longer than that in Case 2, the difference of the convergence speed in  $NRR$  between the FTL algorithms and the VTL algorithms becomes obvious, as shown in Fig. 17. In this case, the VTL algorithms show satisfying convergence rate and performance compared to the FTL algorithms that are simulated under the assumption of a given tap length. From Fig. 18, we can see that VTL-VSS-II

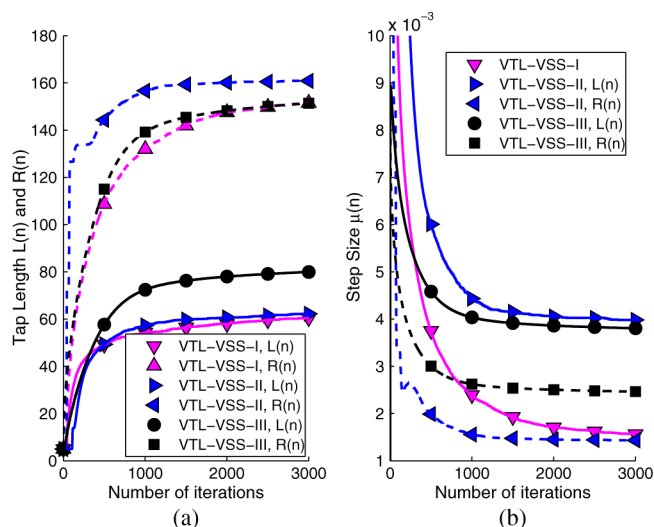


Fig. 18. Convergence of the tap lengths and step sizes for the proposed variable-tap-length algorithm in Case 3. (a) Tap lengths. (b) Step sizes.

also reaches a tap length for  $W(z)$  with about 220 taps while VTL-VSS-I with about 210 taps. Note that, since we do not know the exact tap lengths for  $W^o(z)$  in this case, we set a longer  $M$  and  $N$  in the algorithm. Hence, it is possible for the FTL algorithms to over-estimate the tap length of  $W^o(z)$  slightly for finding minimum MSD with given growth termination parameters  $\kappa_L$  and  $\kappa_R$ . In contrast, The VTL-VSS-III algorithm gives a longer tap length for  $R(n)$  in this case.

## V. CONCLUSION

The conventional fixed-tap-length FxLMS algorithms for ANC usually require a prior long tap-length control filter for different environments, so the convergence rate becomes slow due to the limit of the maximum step size. The new variable-tap-length FxLMS algorithm can self-adjust the required tap length according to the environment such that the new ANC system can better reach fast convergence compared to the conventional FxLMS algorithms. For ANC applications, the primary plant and the secondary path model commonly have unsymmetric impulse responses with respect to the maximum response output. Thus, the new FxLMS algorithm is developed with a generalized form of different step sizes for a two-sided exponential decay response model and is proved to have the minimum MSD for optimal filter coefficients. Some application issues about the proposed algorithm are also addressed in this paper. From the results simulated for the online secondary modeling ANC system, the new variable-tap-length FxLMS algorithm along with different variable step sizes has better convergence rate and performance in contrast to the fixed-tap-length FxLMS algorithms.

## ACKNOWLEDGMENT

The authors would like to thank Prof. Cheng-Yuan Chang, Chung Yuan Christian University, Taiwan for kindly providing audio test models and Prof. Wen-Rong Wu, National Chiao Tung University, Taiwan for cordially giving valuable advice in our research.

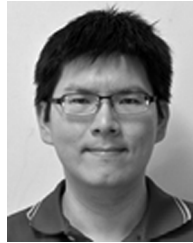
## REFERENCES

- [1] S. J. Elliott and P. A. Nelson, "Active noise control," *IEEE Signal Process. Mag.*, vol. 10, no. 4, pp. 12–35, Oct. 1993.
- [2] S. M. Kuo and D. R. Morgan, *Active Noise Control Systems - Algorithms and DSP Implementations*. New York, NY, USA: Wiley, 1996.
- [3] C.-Y. Chang and S.-T. Li, "Active noise control in headsets by using a low-cost microcontroller," *IEEE Trans. Ind. Electron.*, vol. 58, no. 5, pp. 1936–1942, May 2011.
- [4] S. C. Chan and Y. Chu, "Performance analysis and design of FxLMS algorithm in broadband ANC system with online secondary-path modeling," *IEEE Trans. Audio, Speech, Lang. Process.*, vol. 20, no. 3, pp. 982–993, Mar. 2012.
- [5] R. M. Reddy, I. M. S. Panahi, and R. Briggs, "Hybrid FxRLS-FxNLMS adaptive algorithm for active noise control in fMRI application," *IEEE Trans. Control Syst. Technol.*, vol. 19, no. 2, pp. 474–480, Mar. 2011.
- [6] T. Yucelen and F. Pourboghra, "Kalman filter based modeling and constrained  $H_\infty$  optimal control for active noise cancellation," in *Proc. 46th IEEE Conf. Decision Control*, Dec. 2007, pp. 5401–5406.
- [7] S. M. Kuo and J. Luan, "Cross-coupled filtered-x LMS algorithm and lattice structure for active noise control systems," in *Proc. IEEE Int. Symp. Circuits Syst. (ISCAS '93)*, May 1993, pp. 459–462.
- [8] S. M. Kuo, M. Taherzadeh, and J. Li, "Frequency-domain periodic active noise control and equalization," *IEEE Trans. Speech Audio Process.*, vol. 5, no. 4, pp. 348–358, Jul. 1997.
- [9] S. C. Chan, Y. J. Chu, and Z. G. Zhang, "A new variable regularized transform domain NLMS adaptive filtering algorithm - acoustic applications and performance analysis," *IEEE Trans. Audio, Speech, Lang. Process.*, vol. 21, no. 5, pp. 868–878, Apr. 2013.
- [10] S. J. Park, J. H. Yun, Y. C. Park, and D. H. Youn, "A delayless subband active noise control system for wideband noise control," *IEEE Trans. Speech Audio Process.*, vol. 9, no. 8, pp. 892–897, Nov. 2001.
- [11] M. Wu, X. Qiu, and G. Chen, "An overlap-save frequency-domain implementation of the delayless subband ANC algorithm," *IEEE Trans. Audio, Speech, Lang. Process.*, vol. 9, pp. 1706–1710, Nov. 2008.
- [12] M. T. Akhtar, M. Abe, and M. Kawamata, "A new variable step size LMS algorithm-based method for improved online secondary path modeling in active noise control systems," *IEEE Trans. Audio, Speech, Lang. Process.*, vol. 14, no. 2, pp. 720–726, Mar. 2006.
- [13] A. Carini and S. Malatini, "Optimal variable step-size NLMS algorithms with auxiliary noise power scheduling for feedforward active noise control," *IEEE Trans. Audio, Speech, Lang. Process.*, vol. 16, no. 8, pp. 1383–1395, Mar. 2008.
- [14] B. Huang, Y. Xiao, J. Sun, and G. Wei, "A variable step-size FxLMS algorithm for narrowband active noise control," *IEEE Trans. Audio, Speech, Lang. Process.*, vol. 21, no. 2, pp. 301–312, Feb. 2013.
- [15] G. Long, F. Ling, and J. G. Proakis, "Corrections to 'The LMS algorithm with delayed coefficient adaption'," *IEEE Trans. Signal Process.*, vol. 40, no. 1, pp. 230–232, Jan. 1992.
- [16] S. M. Kuo and D. R. Morgan, "Active noise control: A tutorial review," *Proc. IEEE*, vol. 87, no. 6, pp. 953–973, Jun. 1999.
- [17] M. I. Michalczyk, "Active noise control with moving error microphone," *Mechanics*, vol. 27, no. 3, pp. 113–119, Mar. 2008.
- [18] M. Zhang, H. Lan, and W. Ser, "On comparison of online secondary path modeling methods with auxiliary noise," *IEEE Trans. Speech Audio Process.*, vol. 13, no. 4, pp. 618–628, Jul. 2005.
- [19] M. T. Akhtar, M. Abe, and M. Kawamata, "On active noise control systems with online acoustic feedback path modeling," *IEEE Trans. Audio, Speech, Lang. Process.*, vol. 15, no. 2, pp. 593–600, Feb. 2007.
- [20] M. Wu, X. Qiu, and G. Chen, "The statistical behavior of phase error for deficient-order secondary path modeling," *IEEE Signal Process. Lett.*, vol. 15, pp. 313–316, Oct. 2008.
- [21] L. Wang and W. S. Gan, "Convergence analysis of narrowband active noise equalizer system under imperfect secondary path estimation," *IEEE Trans. Audio, Speech, Lang. Process.*, vol. 17, no. 4, pp. 566–571, May 2009.
- [22] I. T. Ardekani and W. H. Abdulla, "Effects of imperfect secondary path modeling on adaptive noise control systems," *IEEE Trans. Audio, Speech, Lang. Process.*, vol. 20, no. 5, pp. 1252–1262, Sep. 2012.
- [23] Y. Gong and C. F. N. Cowan, "An LMS style variable tap-length algorithm for structure adaptation," *IEEE Trans. Signal Process.*, vol. 53, no. 7, pp. 2400–2407, Jul. 2005.
- [24] Y. Zhang and J. A. Chambers, "Convex combination of adaptive filters for a variable tap-length LMS algorithm," *IEEE Signal Process. Lett.*, vol. 13, no. 6, pp. 628–631, Oct. 2006.
- [25] Y. Zhang, N. Li, J. A. Chambers, and A. H. Sayed, "Steady-state performance analysis of a variable tap-length LMS algorithm," *IEEE Trans. Signal Process.*, vol. 56, no. 2, pp. 839–845, Feb. 2008.

- [26] Y. Gu, K. Tang, H. Cui, and W. Du, "Convergence analysis of a deficient-length LMS filter and optimal-length sequence to model exponential decay impulse response," *IEEE Signal Process. Lett.*, vol. 10, no. 1, pp. 4–7, Jan. 2003.
- [27] Y. Zhang, J. A. Chambers, S. Sanei, P. Kendrick, and T. J. Cox, "A new variable tap-length LMS algorithm to model an exponential decay impulse response," *IEEE Signal Process. Lett.*, vol. 14, no. 4, pp. 263–266, Apr. 2007.
- [28] M. Zhang, H. Lan, and W. Ser, "Cross-updated active noise control system with on-line secondary path modeling," *IEEE Trans. Speech Audio Process.*, vol. 9, no. 5, pp. 598–602, Jul. 2001.



**Dah-Chung Chang** (M'98) received the B.S. degree in electronic engineering from Fu-Jen Catholic University, Taipei, in 1991 and M.S. and Ph.D. degrees in electrical engineering from National Chiao Tung University, Hsinchu, in 1993 and 1998, respectively. In 1998 he joined Computer and Communications Research Laboratories at Industrial Technology Research Institute, Hsinchu. Since 2003, he has been a faculty member in the department of communication engineering at National Central University. His recent research interests include multirate and adaptive digital signal processing, multi-antenna and MIMO communications, and digital transceiver algorithm and architecture design.



**Fei-Tao Chu** was born in Taiwan R.O.C., 1978. He received his B.S. degree in Computer Science and Information Engineering from Chung Hua University, Hsinchu and his M.S. degree in the Institute of Communications Engineering from National Chiao Tung University, Hsinchu, Taiwan in 2013. From June 2000 to January 2012, he served AVID Electronics Corp, ELAN Microelectronics Corp, and WYS SoC Corp. in the research field of audio signal processing. Since 2013, he has worked in Foxlink Image Technology CO., LTD. His research interests include adaptive filtering and active noise cancellation.

License Agreement Subject to IEEE